TASK QUARTERLY 8 No 4, 561–572

DENSITY FUNCTIONAL SIMULATION OF METAL OXIDES: Al_2O_3 AND Fe_3O_4

ZBIGNIEW ŁODZIANA

Institute of Nuclear Physics, Polish Academy of Sciences,
Radzikowskiego 152, 31-342 Cracow, Poland
Center for Atomic-scale Materials Physics,
Department of Physics, DTU,
Building 307, DK-2800 Lyngby, Denmark
Zbigniew.Lodziana@ifj.edu.pl

(Received 6 June 2004; revised manuscript received 17 July 2004)

Abstract: The study of the metal oxides is a rapidly developing area of research. Below a theoretical method based on the density functional theory, common in studying ceramics, is briefly presented. Application of the theory to the surface and the bulk properties of alumina and magnetite are presented. Relaxation mechanism of two different surfaces of alumina and the (100) surface of Fe_3O_4 are shown. The mutual stability of the α and θ phases of Al_2O_3 is calculated.

Keywords: density functional theory, metal oxides, alumina, magnetite

1. Introduction

The electronic structure of metal oxides and metal oxide surfaces is usually well less known than those of metals [1]. This is mainly due to the insulating properties of many metal oxides and their more defective surface structures, which makes experimental techniques more difficult to apply. Thus many basic problems related to the properties of the ceramic surfaces still remain unanswered, despite the fact that this knowledge is strongly desired in the areas of practical use, such as catalysis [2].

In catalysis, metal oxides serve as a support for catalytically active metals (which are often very expensive), or they are catalysts by their own right [2]. These facts reveal the importance of the theoretical description of the metal oxides, and make nowadays theory a complementary method to the experimental techniques in ceramic research.

There are many reasons why we care about a quantum description of ceramics, but probably the most important is that in metal oxides the electronic properties are strongly dependent on the local atomic configuration. Thus semi-empirical methods, which are appropriate for a given atomic environment, often fail to describe properly the structure of one compound in various surroundings, like a bulk and a surface.

Advanced *ab initio* quantum mechanical methods, on the other hand, are computationally too demanding to provide correct structural properties of metal oxides.

Below we briefly illustrate the theoretical description of metal oxides, based on density functional theory (DFT) and give some examples of DFT application to describe the surface properties of aluminum oxide (Al_2O_3) and magnetite (Fe_3O_4). Let's start with a short introduction to problems related to these compounds.

Al_2O_3 is ionio-covalent crystal, which exists in a large variety of structures. The ground state of alumina is known as α-alumina (corundum, sapphire) and it is the second hardest mineral on Earth. It possesses a large band gap of 8eV. Beside the most stable α-phase there exist so called transition phases like: γ, δ or θ alumina. These phases are commonly used as a support material in catalytic industry due to their excellent porosity, which is preserved up to 1300K [3–5]. At the same time the atomic structure of the transition aluminas is very poorly known. The stability of various alumina phases is determined experimentally, but details of the atomic structure of the transition, porous phases is not fully known [6], with exception of the θ-phase. Thus extensive research efforts are focused to elucidate the mechanism governing the porosity and surface structure/properties of alumina. θ-Al_2O_3 is the polymorph, which appears always prior to the transformation to corundum. The best known example is a dehydration process: AlOOH (boehmite) $\rightarrow \gamma \rightarrow \delta \rightarrow \theta \rightarrow \alpha$. At high temperatures ($\sim 1000^{\circ}$C) *spinel based* polymorphs (γ, δ) always coexist with the θ phase, still having good catalytic properties and preserving large surface areas. On the contrary the stable α-phase of alumina is well known single crystal [7] and often serves as a model structure of alumina [8].

In general there are two complex issues related to alumina. One is related to the detailed atomic structure and chemical composition of the transition phases (γ, η, δ, θ polymorphs), another problem is related to the composition and properties of porous alumina surface. As there is no agreement about the bulk structure and composition of porous aluminas, the problems related to the surface are even less understood.

Another problem is related to the metal/metal oxide interface, where properties of such an interface are studied, not least due to their technological importance.

Magnetite Fe_3O_4, crystallizes in the inverse spinel structure with the lattice constant 8.4Å, at room temperature. The Fe ions are localized in two distinct interstitial sites, being octahedraly Fe(B) and tetrahedraly Fe(A) coordinated to oxygen. Above $T \sim 125$K, Fe_3O_4 undergoes an insulator metal transition, thus at room temperature it shows minority spin conductance. The termination and reconstruction of the (100) magnetite surface is still under dispute [9, 10]. This surface is usually discussed in terms of atomic layers of the bulk unit cell. The bulk magnetite consists of subsequent arrangement of the so-called A-layers containing only tetrahedral iron and B-layers which contain oxygen and the octahedral Fe. The layers are separated by about 1.1Å. None of the bulk terminated $Fe_3O_4(100)$ surfaces (neither A nor B) is charge compensated and the charge neutrality condition of the polar $Fe_3O_4(100)$ is quoted as the driving force of the reconstruction. The surface structure, although intensively studied for single crystals [11] as well as for epitaxial films [9], is still not fully understood and explained. The atomic structure of this surface can be probed by scanning tunnelling microscopy [9] due to electric conductance of Fe_3O_4.

The variety of the experimental observations is reflected in many different reconstruction models based on the A- or B-type layer termination proposed and discussed in the literature [9–11]. Two different methods to study this surface are usually employed. One focuses on studies of cleaved bulk crystals [11], whereas another approach relies on thin films grown on the substrate [9]. An observed $(\sqrt{2}\times\sqrt{2})R45^{\circ}$ surface reconstruction is common to both approaches, but it is explained in different manners. The reconstruction is related either to the charge ordering within the B-layer, observed mainly on the bulk magnetite [11], or to reconstruction involving oxygen vacancies within the B-layer [9], nonstoichiometry of the surface termination on the A-layer which is half empty [10] or various displacements of Fe(A) atoms on the octahedral termination.

2. Density Functional Theory

The main problem in surface studies of metal oxides is to resolve the atomic and the electronic structure of the surface. This knowledge provides insight into physico-chemical properties of metal oxides. Theoretical studies of the metal oxides date from the early 20$^{\text{th}}$ century, but models developed up to 20 years ago were based mainly on methods where the atomic interaction was given by a set of phenomenological force constants. Only in a recent years has the development of computational resources given an impact to the so called *ab initio* methods, where the electronic structure is accurately described without any assumed parameters. However, even for the fastest computers, solution of the Schrödinger equation of a many electron system is not possible now, and further simplifications are required. Very successful in the area of *ab initio* calculations is the density functional theory, developed in the mid-sixties by W. Kohn and collaborators [12, 13]. For development of this theory W. Kohn was awarded a Nobel Prize in 1998.

The main idea beyond DFT is to replace N electron many-body problem by the electronic density $\rho(r)$. The self-consistent solution of the appropriate density functional gives the ground state energy of the system.

The large mass difference of electrons and nuclei constituting matter is exploited in the Born-Oppenheimer approximation [14], according to which electrons adiabatically follow the motion of the nuclei. Thus, at any given moment, electrons are in the ground state corresponding to the instant nuclear configuration. The problem of finding the ground state energy of the many-electron system corresponds (in the non-relativistic case) to the time-independent Schrödinger equation:

$$\hat{H}\Psi = \left(\sum_i -\frac{\nabla_i^2}{2} + \sum_{i\neq j} \frac{1}{2|r_i - r_j|} - \sum_{i,J} \frac{Z_J}{|r_i - R_J|} \right) \Psi = E\Psi. \tag{1}$$

The Hamiltonian, $\hat{H}$, includes the kinetic energy of electrons, the electron-electron interactions and the interaction of electrons with the nuclei. The indices i, j run over the electronic degrees of freedom, capital letters are for the nuclei, (atomic units are used throughout). The heart of DFT is the electron density:

$$\rho(r) = \int dr_1 dr_2 \ldots dr_n |\Psi(r_1, r_2, \ldots, r_n)|^2, \tag{2}$$

which is a much simpler quantity than the wave function Ψ, since it depends only on one spatial parameter r. In the numerical representation, either in real or reciprocal space the configuration is represented on a grid, and thus depends only linearly with the system size. The Hohenberg and Kohn [12] theorem is central to DFT and it states that the ground state density of the interacting electrons, which are subject to the external potential $V(r)$ (resulting from the nuclei framework), is a unique function of the electron density. The ground state energy and density can be found by minimizing the energy functional, $E = \min_\rho\{E_V[\rho]\}$:

$$E_V[\rho] = \int dr V(r)\rho(r) + \frac{1}{2}\int dr dr' \frac{\rho(r)\rho(r')}{|r-r'|} + F[\rho]. \tag{3}$$

The appropriate energy functional can be written according to Ref. [12] and it includes three terms: classical Coulomb energy of the electron density distribution ρ, electron interaction with the external potential $V(r)$, and the universal function $F[\rho]$ of the density (independent of $V(r)$) containing all necessary quantities to make the energy equal to the expectation value. $F[\rho]$ include many-body kinetic energy, quantum exchange and correlation effects of the many-electron wave function. The approach formulated in a such way is not very useful, since the explicit expression of $F[\rho]$ is not known. This problem was solved by Kohn and Sham [13], where the concept of the fictitious non-interacting system of electrons having the same density as the real electron gas is introduced. The non-interacting system is described by the orthogonal single particle wave functions $\psi_i(r)$, and the charge density is given by $\rho(r) = \sum_i |\psi_i(r)|^2$, where summation runs over all occupied states. Within this framework the energy functional can be written as:

$$E_V[\rho] = \int dr V(r)\rho(r) + \frac{1}{2}\int dr dr' \frac{\rho(r)\rho(r')}{|r-r'|} + \sum_i \left\langle \psi_i \left| \frac{-\nabla^2}{2}\psi_i \right| \right\rangle + E_{XC}[\rho]. \tag{4}$$

The term which explicitly includes the wave function ψ is the single particle kinetic energy of non interacting electron gas. The last term, $E_{XC}[\rho]$, of the equation is called the exchange-correlation functional, and it contains all contributions (from quantum and kinetic effects) to make it equivalent to the Hohenberg approach. The fact that in the last equation the wave functions are present explicitly is not a real complication, as the appropriate Euler-Lagrange equation can be solved to minimize the energy functional.

DFT theory is in principle exact, but since the form of the exchange-correlation ($E_{XC}[\rho]$) functional is not known, various approximations are used. Historically the first and surprisingly accurate approach is called the local density approximation (LDA). The idea behind it is to replace the non-local functional by a functional that depends only locally on the electronic density of the uniform electron gas: $E_{XC}[\rho] = \int dr \rho(r)\varepsilon_{XC}(r) = \int dr \rho(r)\varepsilon_{XC}(\rho_{hom}(r))$. The exchange and correlation energy of the homogenous electron gas is well known [15]. The LDA approximation gives the structural parameters within 1–2% for ceramics, but the cohesive or atomization energies are usually much worse (around 20–30%) [16]. The logical extension of the LDA is to include variation of the electron density in the exchange-correlation functional $E_{XC}[\rho] = \int dr \rho(r)\varepsilon_{XC}(\rho(r), \nabla\rho(r))$. This is known as the generalized gradient approximation (GGA) [17]. When GGA approximation is formulated in a way to fulfill

general limit requirements for the electron gas, the accuracy of DFT improves significantly. The gradient corrected approach is still semi-local and does not include any kinetic effects. Development of the theory nowadays aims toward more accurate exchange-correlation functionals, which also include many body kinetic effects [18]. Another approach, very popular in a chemistry community, is to resign from rigorous limit conditions for the electron gas and construct exchange-correlation functionals by fitting their properties to the experiments (on light noble gas atoms). In that way new functionals might be constructed, which can also include exact exchange energy.

From a practical point of view the wave functions have to be expanded in an appropriate basis set. Two types of basis sets are the most popular: the localized basis (with gaussian type orbitals), and the plane wave expansion, where basis set consists of the plane waves in a periodic unit cell. The later approach is very appropriate for crystalline materials, where periodic boundary conditions are natural. Delocalization of the electrons is very easily obtained within this approach. A localized basis set, on the other hand, is more appropriate for molecular systems (it can be also more accurate), however structural relaxation cannot be easily described in this formalism.

More details about the method can be found in the excellent review paper [19] or monograph [20].

2.1. Beyond the lattice ground state

DFT calculations provide information about the ground state properties of matter, while one is often interested in the thermodynamic functions at finite temperatures. This can be obtained by calculations of the free energy, based on the quasiharmonic approximation [21].

Among many methods to calculate lattice vibrations, one was developed in the group of Prof. K. Parliński in Cracow. The so called direct method [22] is fully based on DFT calculations of the atomic forces in a real space. The dynamical matrix is constructed for the supercell, consisting of multiple unit cells of the structure under investigation. The method utilizes the Hellman-Feynmann forces acting on atoms in the supercell, which are determined by a series of independent displacements along x, y, z directions for every symmetry nonequivalent atom. Next, the symmetry of the force constants, following from the particular space group of the investigated material is established. The force constants are fitted to the collected Hellmann-Feynman forces by the singular value decomposition method. When at a given distance the largest element of the force constant is more than three orders of magnitude smaller than the corresponding one from the first shell the size of the supercell is sufficient for the reliable results. The diagonalization of the dynamical matrix provides the phonon frequencies.

The method is correct for the analytical part of the dynamical matrix only, as periodic boundary conditions are imposed on the supercell. The large band gap of most oxides causes incomplete screening, reflected by the Born effective charges carried by ions. Thus, the nonanalytical part of the dynamical matrix, which describes the effects of this macroscopic electrostatic field for certain infrared (IR) modes in the long wavelength limit ($\mathbf{q} \to 0$) has to be taken into account. A Coulomb interaction splits these modes into longitudinal (LO) and transversal (TO) parts, lifting the LO-TO degeneracy. The method accounts for the nonanalytical part of dynamical matrix

by introducing the effective charges of the ions. They can be calculated separately or a special technique with elongated supercells need to be applied. The independent elements of the dielectric tensor must also be known. More details of this method are presented elsewhere [23].

2.2. Implementation of DFT

Numerical implementation of DFT is a complex issue that requires coding of more than 20000 lines. At present there exist many excellent realizations of DFT, which provide easy, ready to use tools to study the electronic and structural properties of the metal oxides. To mention only some the interested reader may refer to the GPL codes like: DACAPO [24], ABINIT [25], SIESTA [26]. Some other excellent codes are unfortunately not free: VASP [27], WIEN2K [28]. Most implementations are done in the plane wave formalism [24, 25, 27].

Efficiency is an important factor to determine whether DFT code is applicable to a given problem. In general plane wave representation of the wave functions scales as $O(M^3)$, where M is the number of points of the grid (proportional to the number of electrons or size of the system). Accurate calculations can be carried up to several hundred light atoms on parallel platforms. There are implementations, with localized basis sets, which allows linear scaling $O(M)$ [26]. With rapid expansion of the parallel computing approach based on the real space representation of the wave function is a very promising alternative to the methods based on the reciprocal space representation.

2.3. Important points for calculations of metal oxides

Despite the broad code availability, the simulations of the metal oxides require some caution. Below some crucial aspects that have to be considered prior to the interpretation of the results are listed.

The choice of the exchange-correlation functional is crucial for the final results. If one is interested in a crude structural properties, the LDA approximation is often sufficient. In most other cases the functionals that go beyond LDA are required. For description of the chemical processes at the surfaces LDA is inappropriate, since it poorly describes the atomic bonding.

The all-electron wave functions of atoms are usually replaced by the so-called, pseudopotentials. The pseudopotential replaces the inert core electrons, so only chemically active valence electrons are explicitly represented. This approach has proven to be accurate in the description of the ceramics [6]; some care must be taken, however, to assure that the appropriate pseudopotential is chosen. In general ultrasoft pseudopotentials [29] are appropriate for metal oxides because only valence electrons contribute to the ionic bonding. For systems which include transition metals, the projector augmented-wave [30] (PAW) potentials might be a better choice, because the charge density in the core region is described more precisely in this formalism. The core-valence coupling can also be important for transition metal oxides. PAW potentials are also necessary for calculations employing sophisticated exchange-correlation functionals, or systems with strong correlations of the electron gas.

For the systems containing strongly correlated electrons, like NiO, the DFT method needs to be extended, and Hubbard-like models must be added to the

formalism [31]. An alternative approach is to use self-interaction corrections [32] in the DFT formalism. Both approaches improve calculated band gap and electron localization, although advanced Hartree-Fock methods are sometimes more versatile in this case.

Weak interactions, especially Van der Waals type, are not properly described within the present quantum theories. This is due to strongly non-local character of the E_{XC} functional, which is responsible for this type of interactions [33]. For that reason special precautions have to be taken for systems where this type of interaction is important, like V_2O_3.

The atomic structure observed experimentally by scanning tunnelling microscopy (STM) can also be described within the DFT formalism. Theoretical analysis of the STM topographs are based on Tersoff-Hamann formalism [34]. Within this formalism the tunneling current simply reflects the iso-surface of the local density of states at the Fermi level $\rho(R,\epsilon_F)$, where R is a position of the tip. To account for the final sampling of the Brillouin zone the energy levels are replaced by Gaussians with a finite width. In many cases calculations are crucial for proper interpretation of the observed atomic patterns on metal oxides. Unlike metals for ceramics increased charge density is not always related to the presence of atoms.

3. The model and calculation setup

Application of DFT to study properties of the metal oxides is illustrated below by a set of results, which provide explanation of some problems related to both the bulk and the surface. The following model was used.

The structures and the dynamics of Al_2O_3 and Fe_3O_4 were calculated within DFT approach [24, 27]. The ionic cores are represented by ultra soft pseudopotentials. The electronic density is determined by iterative diagonalization of the Kohn-Sham Hamiltonian and the resulting Kohn-Sham eigenstates are populated according to the Fermi statistics with finite temperature smearing of $kT = 0.02\,\mathrm{eV}$. For magnetite the smearing temperature was $kT = 0.005\,\mathrm{eV}$. Pulay mixing of the resulting densities is applied and the procedure is repeated until a self-consistency of electronic density is achieved. Then the total energy is extrapolated to $T = 0\,\mathrm{K}$. The calculations were carried within GGA PW91 [17] approximation of the exchange correlation functional. Very restrictive accuracy was applied to compare the relative stability of α and θ phases of alumina at $T = 0\,\mathrm{K}$. The wave function was sampled according to a Monkhorst-Pack scheme with k-point density of $0.05\,\mathrm{\AA}^{-1}$ to $0.02\,\mathrm{\AA}^{-1}$. For the calculations of the lattice dynamics, larger supercells were used to assure the force constants fell sufficiently with distance. The calculations were performed on systems of up to 120 atoms. The cutoff of the kinetic energy was 490eV. The structure was optimized according to the calculated Hellmann-Feynman forces. Both internal positions of atoms and the unit cell parameters were optimized.

The surface calculations were performed in a slab geometry for both Al_2O_3 and Fe_3O_4. The vacuum region extends from 12Å, to 20Å. The middle atomic layer of the slab was fixed in the bulk configuration, and both surfaces of the slab were relaxed. The binding energy of Pd on alumina is calculated with respect to the gas phase of palladium.

4. Applications

Below we present examples from our own studies for both the bulk metal oxide and the surfaces.

The first example of DFT application concerns the interaction of palladium atoms with the (0001) surface of corundum. There are two objectives of this research: to describe properly the surface structure of α-alumina and to determine the mechanism and energy of metal/surface interaction [35]. The (0001) surface of corundum consists of layers of cations and anions aligned in the planes parallel to the surface. It undergoes very large relaxation, that requires careful choice of the model. The ideal surface is terminated by a single Al layer, although other terminations were also reported in the literature [8]. They consist of various degrees of surface hydroxylation, or under very low oxygen pressure, termination by the oxygen layer.

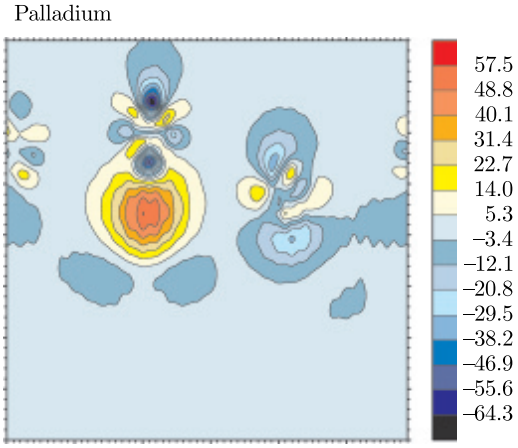

Figure 1. The charge density difference Pd/corundum interface; the dark negative values indicate charge depletion, positive values are for the charge accumulation

In Figure 1, a map of charge density is presented, which shows polarization of the Pd orbitals. One monolayer of palladium is put on the stoichiometric surface of corundum and the interface is fully relaxed. The polarization of Pd orbitals indicate that the interaction of the Pd monolayer with the relaxed surface of corundum is mainly of the electrostatic nature; no charge transfer is observed. The adsorption energy, for Pd monolayer is of the order $1\mathrm{J/m}^2$. The interaction of Pd with other surface terminations is significantly stronger [35] (up to $5\mathrm{J/m}^2$), thus indicating that metal atoms would bind preferentially to defects on the surface.

The surface relaxation (and the surface energy) is related to charge transfer between the ions and the oxide structure extending from the surface deep into the bulk. Alumina, which possesses a large variety of structures, is a good example to study charge transfer related to the coordination change of the ion at the surface [8]. Trigonal α and monoclinic θ-phases have different distribution and coordination of Al cations, and substantial differences in the surface relaxation mechanisms are expected. In corundum only octahedrally coordianted Al cations are present, while in θ-alumina 50% of Al cations have tetrahedral coordination. It is presented in Figure 2, that despite very different bulk atomic structures in the surfaces of considered phases of

alumina, the mechanism of the charge transfer is very similar. The charge transfer is related to the substantial relaxation of the surface, where the surface atoms can be displaced by 0.07nm. This relaxation extends deep into the bulk, so the proper description of the surface requires rather large systems often containing ∼100 atoms.

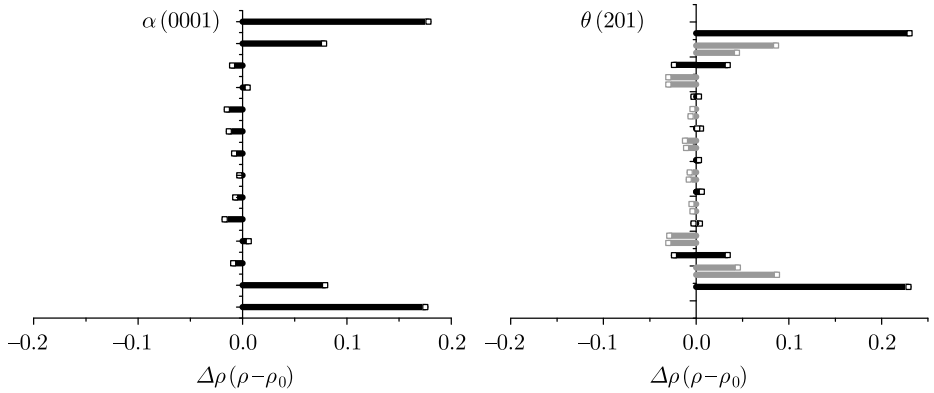

Figure 2. The change of the valence electronic charge of Al cations with respect to the bulk charge of the (0001) surface of α-Al_2O_3 and (201) face of θ-Al_2O_3; the vertical axis represents the direction perpendicular to the surface, such that the top and the bottom bars are for the surface atoms; the center of the slab is in the middle of the vertical axis; light bars are for octahedral cations, dark bars represent tetrahedrally coordinated cations in θ-Al_2O_3; positive values indicate charge accumulation

Knowledge of the electronic and the structural properties of the surface allows calculation of topographic effects like STM images. This is shown in Figure 3, where theoretical STM image of B-layer terminated (100) surface of magnetite is presented.

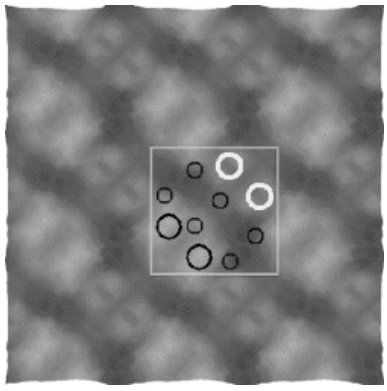

Figure 3. The calculated STM topograph of the (100) surface of magnetite; bright colors correspond to larger electronic density (higher tunnelling current); the square in the middle represents the reconstructed $(\sqrt{2}\times\sqrt{2})R45^\circ$ surface unit cell; large circles are for surface iron cations, small represent surface oxygen; dark and light Fe are structurally equivalent, but charge ordering at the surface is clearly visible distinguishing two types of Fe

The DFT calculations reveal only minor structural rearrangements of the B-plane termination, however, leading to the significant changes in the electronic structure of the surface. The generally ionic, high spin character of the bulk is

preserved at the surface. The most important change is differentiation of the local spin moments on Fe(B) giving rise to ordering of the octahedral cations at the surface. Pairs of cations with $\mu_{B1} = 3.50\mu_B$ and $\mu_{B2} = 2.74\mu_B$ are formed. The changes of the magnetic moments on Fe(B) cations are related to the ordering of electrons on atomic orbitals. Strong interaction between the oxygen p-band, which approaches iron, and d-electrons of Fe(B) repulses them away from the top of the valence band into conduction band above the Fermi level. The calculated electronic structure of the octahedral termination of the (100)-Fe_3O_4 indicates a charge ordering and allows association of the observed surface $(\sqrt{2}\times\sqrt{2})R45^\circ$ reconstruction to the ordering of the Fe charges, rather than to the structural relaxation of the surface. Theoretical STM images can be directly compared to the experimental ones and the agreement is very good [36]. Theoretical calculations allow study of the real underlying atomic structure of the surface.

The final example shows the comparison of the bulk free energy for the α and θ-phases phases of alumina at finite temperature. This requires calculations of the lattice dynamics and comparison of the free energy contributions resulting from the phonons. The vibrational density of states was determined by a direct method [22] for both phases of alumina and the free energy was calculated according to the quasiharmonic approximation. The difference of the free energy is presented in Figure 4. In agreement with the experiment α-alumina is a ground state at low temperatures [37]. With increasing temperature this phase is destabilized in favor of θ-alumina, but the vibrational contribution alone is too weak to drive the phase transformation below the melting point of Al_2O_3. The result indicates that there must exist an additional mechanism, which stabilizes porous form of θ-alumina below 1300K. It was suggested that this mechanism can be related to the lower surface energy of the transition phases [4]. The surface energy of θ-phase is indeed lower than those of corundum ($0.8\mathrm{J/m^2}$ vs. $1.8\mathrm{J/m^2}$, respectively), but this does not explain thermal stability of the porous alumina phases. It was shown recently, that the surface of porous θ-alumina can have negative surface energy, while it stays hydroxylated [5]. In this perspective the porous phase is nothing unusual and shall be stable as long as the surface is hydroxylated.

5. Summary

Theoretical aspects of density functional theory are briefly presented with a few examples of its practical implementation. Some important issues related to DFT modelling of the metal oxides are stressed. Application of the theory to modelling of the metal oxides is illustrated with four examples. Two examples concern the surface properties of alumina, and binding energy of Pd/corundum (0001) facet. It is shown that the electrostatic polarization is the main mechanism of the interaction between palladium monolayer and (0001) surface of corundum. The surface relaxation mechanism is very similar for different structural forms of alumina. The next example shows theoretical STM image of the octahedral termination of the (100) face of magnetite. This can be compared directly to the experiment and reveal the charge ordering as a main mechanism of the surface reconstruction. The last example concerns mutual stability of the α and θ phases of alumina. The difference of the bulk

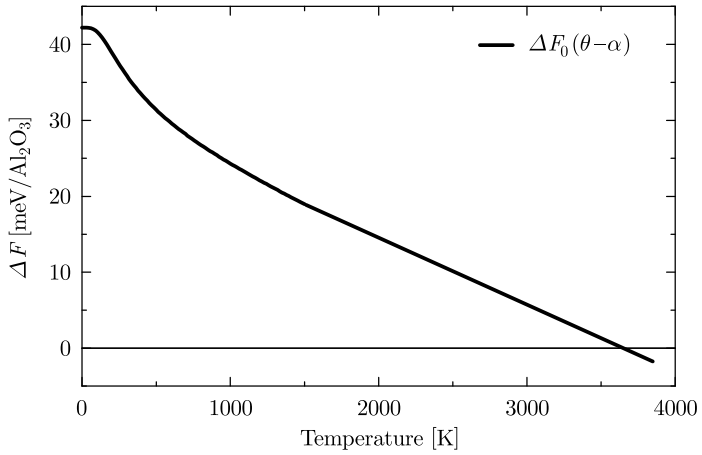

Figure 4. The difference of the free energy $\Delta F = \Delta E_0 - T\Delta S$, between α and θ phases of Al_2O_3

free energy between these phases of alumina is calculated and it indicates that the α-phase always possesses lower free energy up to the melting point when crystalline bulk material is considered.

Acknowledgements

The author would like to thank Dr. N. Bailey for reading the manuscript. Simulations were run on computing power at the Academic Computer Centre CYFRONET-Cracow, grant KBN/SGI/IFJ/061/2002 and KBN/SGI_ORIGIN_2000/IFJ/150/1998.

References

[1] Heinrich V E and Cox P A 1994 *The Surface Science of Metal Oxides*, Cambridge University Press
[2] Freund H-J 2002 *Surf. Sci.* **500** 271
[3] Wefers K and Misra C 1987 *Oxides and Hydroxides of Aluminium*, Alcoa Techincal Paper (19), Alcoa Laboratories (revised)
[4] McHale J M, Auroux A, Perrota A J and Navrotsky A 1997 *Science* **277** 788
[5] Łodziana Z, Topsøe N-Y, and Nørskov J K 2004 *Nature Mat.* **3** 269
[6] Wolverton C and Hass K 2001 *Phys. Rev.* **B 63** 24102
[7] Hass K C, Schneider W F, Curioni A and Andreoni W 1998 *Science* **282** 265
[8] Łodziana Z, Nørskov J K and Stoltze P 2003 *J. Chem. Phys.* **118** 11179
[9] Stanka B, Hebenstreit W, Diebold U and Chambers S A 2000 *Surf. Sci.* **448** 49
[10] Kim Y J, Gao Y and Chambers S A 1997 *Surf. Sci.* **371** 358
[11] Mariotto G, Murphy S and Shvets I V 2002 *Phys. Rev.* **B 66** 245426
[12] Hohenberg P and Kohn W 1964 *Phys. Rev.* **B 136** 864
[13] Sham L J and Kohn W 1965 *Phys. Rev.* **A 140** 1133
[14] Born M and Oppenheimer J R 1927 *Ann. Physik* **84** 457
[15] Ceperly D M and Adler B J 1980 *Phys. Rev. Lett.* **45** 566
[16] Kurth S, Perdew J P and Blaha P 1999 *Int. J. Quantum Chem.* **75** 889
[17] Perdew J P, Chevary J A, Vosko S H, Jackson K A, Pederson M R, Singh D J and Fiolhais C 1992 *Phys. Rev.* **B 46** 6671
[18] Mattson A E 2002 *Science* **298** 759
[19] Kohn W and Vashista P 1983 *General Density Functional Theory*, in Lundquist S and March N H *Theory of the Inhomogenous Electron Gas*, Plenum Press, pp. 79–147
[20] Parr R G and Wang W 1989 *Density-Functional Theory of Atoms and Molecules*, Oxford University Press, Oxford

[21] Ackland G J 2002 *J. Phys.: Condens. Matter* **14** 2975
[22] http://wolf.ifj.edu.pl/phonon/, Computer code PHONON (Cracow, Poland 2004)
[23] Parliński K, Li Z Q and Kawazoe Y 1997 *Phys. Rev. Lett.* **78** 4063
[24] http://www.fysik.dtu.dk/campos/Dacapo/
[25] http://www.abinit.org/
[26] Soler J M, Artacho E, Gale J D, García A, Junquera J, Ordejòn P and Sànchez-Portal D 2002 *J. Phys.: Condens. Matter* **14** 2745,
http://www.uam.es/departamentos/ciencias/fismateriac/siesta/
[27] Kresse G and Furthmüller J 1996 *Comput. Mater. Sci.* **6** 15,
http://cms.mpi.univie.ac.at/vasp/
[28] http://www.wien2k.at/
[29] Vanderbilt D 1990 *Phys. Rev.* **B 41** 7892
[30] Blöchl P E 1990 *Phys. Rev.* **B 41** 5414
[31] Antonov V N, Harmon B N, Antropov V P, Perlov A Y and Yaresko A N 2001 *Phys. Rev.* **B 64** 134410
[32] Perdew J P and Zunger A 1981 *Phys. Rev.* **B 23** 5048
[33] Dion M, Rydberg H, Schröder E, Langreth D C and Lundqvist B I 2004 *Phys. Rev. Lett.* **92** 246401
[34] Tersoff J and Hamann D R 1983 *Phys. Rev. Lett.* **50** 1998
[35] Łodziana Z and Nørskov J K 2001 *J. Chem. Phys.* **115** 11261
[36] Łodziana Z and Korecki J 2005 (in preparation)
[37] Łodziana Z and Parliński K 2003 *Phys. Rev.* **B 67** 174106